



21, rue d'Artois, F-75008 PARIS

<http://www.cigre.org>

CIGRE US National Committee 2019 Grid of the Future Symposium

Successful Site Acceptance Tests for Microgrid-Integrated Battery Energy Storage

M. BAZRAFSHAN, A. MAJZOABI, A. KHODAEI
University of Denver
USA

N. GURUNG, H. CHEN, L. ZHANG, M. LELIC, A. VALBUENA GUERRA
Commonwealth Edison
USA

SUMMARY

ComEd is in the process of building the first-ever microgrid cluster in the world, within the Bronzeville neighborhood of Chicago. This cluster will connect the Illinois Institute of Technology (IIT) campus microgrid to the newly-developed Bronzeville Community Microgrid (BCM). Besides the focus on investigating cluster control and operations, one of the primary goals of the BCM project is to address the inherent power fluctuations of solar photovoltaic (PV) technologies by coordinating energy storage and leveraging ancillary services of smart inverters connected to PV and storage systems. To this end, a utility-scale battery energy storage system (BESS) and multiple rooftop PV systems have been installed in BCM. This paper presents analyses of interesting site acceptance test (SAT) for the BESS. The SAT is required to ensure that the installed controllers adjoined with protection and communication units can control the BESS so that the BCM complies with interconnection standards.

KEYWORDS

Battery Energy Storage, Solar Photovoltaic, Microgrid, Site Acceptance Test

This material is based upon work supported by the U.S. Department of Energy's Office of Energy Efficiency and Renewable Energy (EERE) under Solar Energy Technologies Office (SETO) Agreement Number EE0007166.

amin.khodaei@du.edu

INTRODUCTION

Microgrids are anticipated to be one of the major components of future power grids. Microgrids aid power system reliability and resilience, allow for the integration of clean renewable energy, and facilitate electricity access to distant areas not served with centralized grids [1]. Microgrid components include distributed energy resources such as solar PV and battery systems, master controllers, and smart inverters [2]. Not only these local resources can be controlled to simulate a flexible demand for the utility grid, a microgrid further can disconnect from the utility grid in case of disturbances [3].

Indeed, such flexibilities are reliant upon a seamless hierarchical control over microgrid constituents that would, for instance, allow curbing the variability of renewable energy and demand. An explicit example is an operation of battery energy storage systems (BESSs) that may be leveraged to store the output of solar PV systems in periods of high production, and further delay the power discharge during periods of low generation and high-power demand. This concept forms the basis of many recently developed PV-battery control hierarchies [4], [5], [6].

One of the primary goals of the recently launched microgrid by ComEd in the Bronzeville neighborhood in the south side of Chicago [7] is to address the inherent fluctuation of PV production by incorporating BESS reinforced with ancillary capabilities of smart inverters. To this end, both PV and BESS systems have been installed in the Bronzeville Community Microgrid (BCM). The PV system entails rooftop installations on 17 buildings and amounts to a nominal capacity of 484 kW AC, with a DC capacity of approximately 587 kW which is controlled and communicated with via a single point of connection. The BESS unit is a utility-scale front-of-meter 500 kW/2000 kWh DC-AC system.

The one-line diagram of the BCM is depicted in Figure 1. Switch 1 indicates the point of connection of BCM to the upstream grid. The PV system is connected via switch 3 to BCM. The additional PV system from Illinois Institute of Technology on the diagram is disconnected from BCM as switch 4 is normally open. To ensure that the operation of the BCM complies with interconnection standards and that BESS and smart functionalities of inverters can be utilized to alleviate adverse effects of PV fluctuation, a series of tests must be conducted on both BESS and PV systems. Successful passing of the SAT indicates the potential of system controllers jointly with protection and communication units to implement advanced algorithms that continuously maintain BCM operation in compliance with interconnection standards.

This paper presents analyses pertaining to several tests as part of the SAT conducted for the BESS system. In Sections 2, 3, and 4 we present three interesting tests for BESS which comprise the P/Q Priority Test, Volt/VAR Control Test, as well as Power Factor Control Test. The paper concludes in Section 5 with pointers to future work.

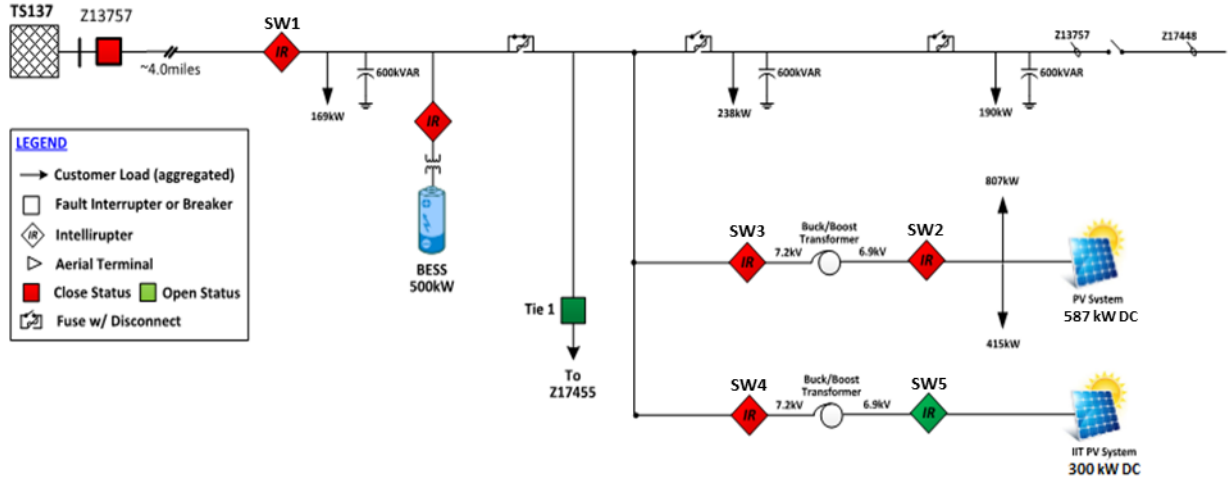


Figure 1. One-line diagram of BCM.

1. P/Q PRIORITY TEST

The purpose of the P/Q priority test is to ensure that the BESS can give higher priority to either its real power output or its reactive power output if commanded to do so. The priority test adjusts an input called the priority signal. When the priority signal is set to real power, the inverter controller is prompted to follow the real power setpoint. When the priority is set to reactive power, the inverter controller is prompted to follow the reactive power setpoint. If the inverter reaches its apparent power capacity, the quantity that is not prioritized will be curtailed.

The results of this test are plotted in Figure 2. The horizontal axis represents the local time. The vertical axis on the left represents power in kW, reactive power in kVAR or apparent power in kVA. The vertical axis on the right depicts the unitless priority signal. Priority signal of 1 implies that the priority is with the BESS real power while the priority signal of 2 implies that the priority is with the reactive power. The dashed lines are indicative of a command signal and the solid lines are indicative of measurements.

At the start of the test, i.e., from 1:00:00 to 1:09:45 p.m., the priority signal is set to 1 implying that the BESS real power output will be prioritized. Before 1:02:10 p.m., the BESS reactive power setpoint is zero and thus no reactive power is produced by the BESS. In this time, the BESS real power output follows the real power setpoint of 500 kW and ultimately the apparent power output of the BESS remains at 500 kW.

After 1:02:10 p.m. but before 1:09:45 p.m., the reactive power setpoint of BESS is set to 400 kVAR. However, since the apparent power capacity of BESS is about 600 kVA and that the priority is with real power output, the reactive power output cannot reach 400 kVAR and is curtailed. The reactive power output can only theoretically reach the following value of

$$Q_{max} = \sqrt{S_{nominal}^2 - P_{measured}^2} = \sqrt{600^2 - 500^2} \approx 331.66 \text{ kVAR.}$$

Indeed, in this time interval, the BESS reactive power output depicted in Figure 2 is close to the value computed above which indicates that it has been curtailed from the setpoint of 400 kVAR. This verifies the portion of the P/Q priority test of real power priority.

From 1:09:45 p.m. to 1:36:50 p.m., the priority signal is set to 2 implying that the BESS reactive power output will be prioritized. In this time interval, but before 1:10:50 p.m., the real and reactive power setpoints are fixed, respectively at 100 kW and 400 kW. Since the resulting apparent power computed from these setpoints equals 412.31 kVA and is less than the nominal BESS size of 600 kVA, both real and reactive power outputs follow their corresponding setpoints of 100 kW and 400 kVAR, respectively.

After 1:10:50 p.m. but before 1:36:50 p.m., the real power setpoint is set to 500 kW. In this time interval, the resulting apparent power computed from the real and reactive power setpoints surpasses the nominal BESS size of 600 kVA. Consequently, since the priority signal is set to reactive power, the real power output of the BESS must be curtailed. The real power output in this time interval can only theoretically reach the value of:

$$P_{max} = \sqrt{S_{nominal}^2 - Q_{measured}^2} = \sqrt{600^2 - 400^2} \approx 447.21 \text{ kW}.$$

Indeed, in this time interval, the BESS real power output depicted in Figure 2 is close to the value computed above which indicates that it has been curtailed from the setpoint of 500 kW. This verifies the portion of the P/Q priority test of reactive power priority. After 1:37:55 p.m. the test terminates and the priority signal is set to 0 indicating a priority for neither the real nor the reactive power setpoints.

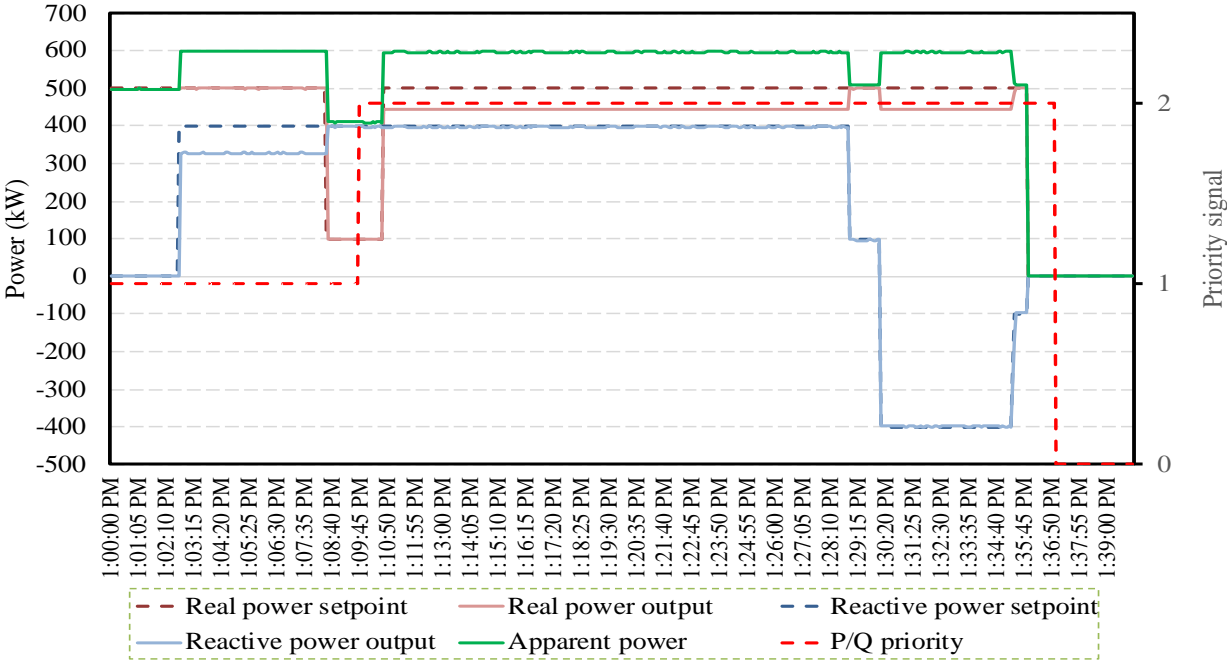


Figure 2. P/Q priority tests.

When the priority signal is set to real power, reactive power output will be curtailed if the resulting apparent power computed from real and reactive power setpoints exceeds the nominal apparent power capacity of BESS. When the priority signal is set to reactive power, real power output will be curtailed if the resulting apparent power computed from real and reactive power setpoints exceeds the nominal apparent power capacity of BESS.

2. VOLT-VAR CONTROL TEST

The purpose of this test is to evaluate the reactive power capabilities of the BESS in response to voltage variations. The charge and discharge real power setpoints of the BESS are leveraged to deliberately affect the voltage at the Point of Connection (POC). When the BESS inverter is in the Volt-var control mode, its reactive power output will vary according to a specific Volt-var curve to alleviate voltage deviations beyond acceptable limits.

A four-point Volt-var control curve is provided in Figure 3. This Volt-var curve is at the disposal of BESS inverter which identifies three operating regions for the inverter. When the POC voltage is low, i.e., between 50percent to 99percent of the nominal value, the reactive power *injection* of the BESS is at 80percent of its kVA size. On the other hand, when the voltage is high, i.e., between 101percent to 150percent of its nominal value, the reactive *consumption* of the BESS is at 80percent of its kVA size. When the voltage is within a 1 percent range of its nominal value, i.e., when its value is within 99percent to 101percent of its nominal value, the reactive power output of the BESS varies linearly with a 48000 kVAR/pu slope.

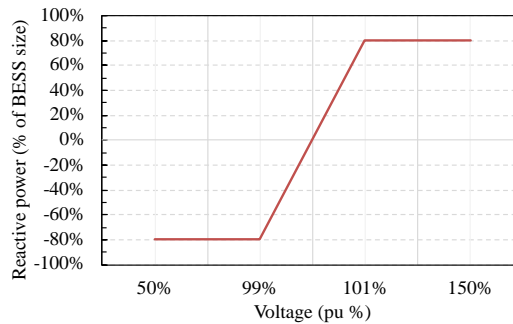


Figure 3. A four-point Volt-var curve

The successful application of the four-point curve is demonstrated in Figure 4. In this figure, a positive value of real power implies discharging or *injection* from the battery while a negative value implies charging or *consumption*. On the other hand, a positive value of reactive power implies consumption and a negative value implies injection. Before the start of the test, at 5:40:00 p.m., a reactive power setpoint is set to 300 kVAR consumption so that voltages drop below 0.99 pu. The Volt-var control mode of the inverter is turned on just before 5:41:30 p.m.. Upon exerting this trigger, the reactive power ceases to follow its setpoint. Rather, since the voltage is below 0.99 pu, the reactive power consumption reduces, to ideally reach 80 percent of its kVA size. As the reactive power consumption reduces, the voltage bounces back to within the 1percent deviation from the nominal value causing the reactive power to stay within 100 kVAR. When the voltage is within 1percent deviation from its nominal value, the reactive power output of the inverter varies according to the linear regime in the left-hand-side of Figure 3. Since the slope is high, i.e., 48000 kVAR/pu, the variations of reactive power seem more apparent in Figure 4 but tiny voltage variations are not visible because the resolution of the data is 1V. A consistent drop of reactive power consumption ending at 5:48:00 p.m. prompts a fairly small voltage rise. At 5:49:00 p.m. the *real* power setpoint is intentionally increased from 0 kW to 100 kW and then dropped to -500 kW, to cause voltage fluctuation. The reactive power consumption subsequently fluctuates but overall decreases. The reactive power *injection* at 5:50:00 p.m. prevents voltages from dropping below 0.99 pu. At 5:52:00 p.m., the Volt/VAR

control mode is turned off. The reactive power injection increased prompting voltage to rise by 5:53:30 p.m..

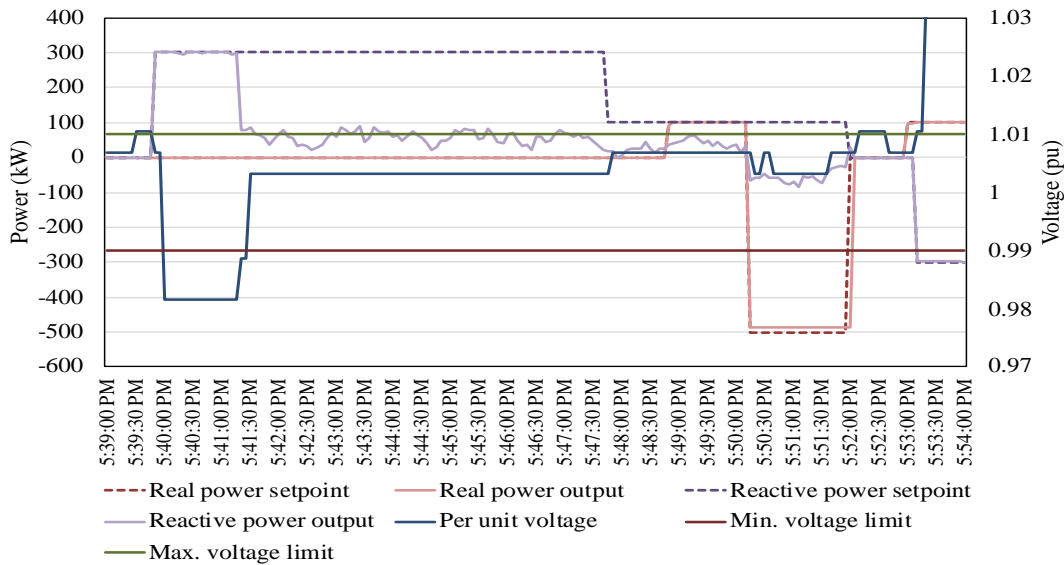


Figure 4. Successful application of Volt-var control using a four-point curve

3. POWER FACTOR CONTROL TEST

The power factor control test is conducted to verify the ability of the BESS inverter to follow a leading and lagging power factor setpoint. When the BESS is set to power factor mode, its reactive power is adjusted automatically so that regardless of the BESS real power output, the BESS power factor reaches its given setpoint. In the analysis below, the power factor is measured according to the following:

$$pf = \text{sign}(q) * \frac{p}{\sqrt{p^2 + q^2}} \quad (1)$$

Where p and q are respectively the BESS real and reactive power measurements. In the above equation $\text{sign}(0)$ is interpreted to be 1. The sign of the reactive power output, q , is included in equation (1) to enable us to accommodate both lagging and leading power factors in the same figure. A positive pf from (1) implies a lagging power factor and a negative pf from (1) implies a leading power factor.

Successful result of this test is demonstrated in Figure 5. The real power and the power factor setpoints are initially set to 300 kW discharge and unity respectively. In this initial setup, the reactive power output of the BESS inverter stays at 0 kVAR. At about 1:54:25 p.m., the power factor setpoint of the inverter is set to 0.9. Following this command, the reactive power consumption of the inverter reaches 144 kVAR by 1:55:15 PM; a departure from its setpoint. Notice that by substituting the values of 300 kW and 144 kVAR in place of p and q in (1), the resulting power factor is found to be 0.901 which is equal to the power factor setpoint.

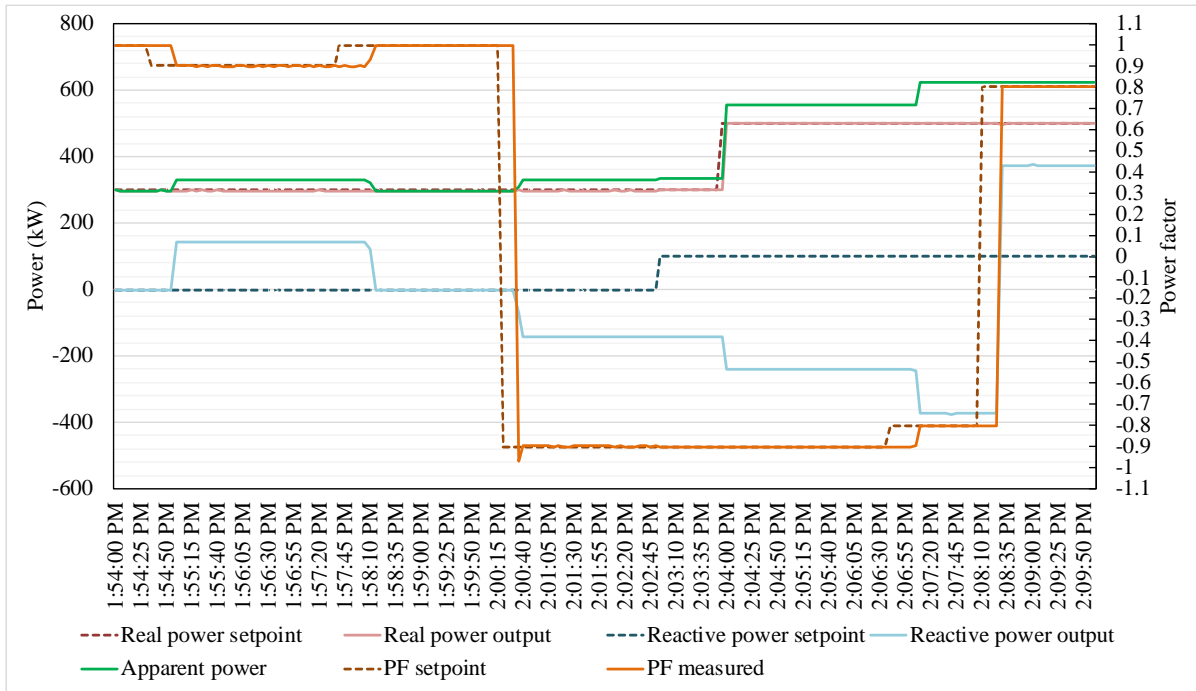


Figure 5. Successful result of the power factor control test.

At 1:57:45 p.m. the power factor setpoint is set back to unity. By a small delay, at 1:58:10 p.m., the reactive power output of the inverter goes back to 0 to ensure that the power factor measured conforms to the unity power factor command. At 2:00:15 p.m., the power factor setpoint is changed to 0.9 leading. Subsequently, the reactive power *injection* of the inverter reaches 144 kVAR at 2:00:40 p.m. to ensure that the power factor computed from (1) conforms to 0.9 leading. Recall that in Figure 5, negative reactive power indicates injection.

At 2:02:45 p.m., the reactive power setpoint of the inverter varies. Nevertheless, the reactive power output of the inverter neglects this command as the inverter is set to power factor control mode. At 2:04:00 PM, the real power setpoint and subsequently the real power discharge of the BESS inverter change to 500 kW. The reactive power injection of the inverter automatically adjusts to 240 kVAR. From (1), we observe that $p = 500$ and $q = -240$ ensure a 0.9 power factor leading.

At 2:06:30 p.m., the power factor setpoint changes to 0.8 leading. With a slight delay, at 2:07:20 p.m., the reactive power injection changes to 372 kVAR to ensure a 0.8 power factor leading. At 2:08:10 p.m., the power factor setpoint changes to 0.8 lagging. With a slight delay, the reactive power output varies from injection at 372 kVAR to consumption at 372 kVAR to conform to the power factor of 0.8 lagging.

4. CONCLUSIONS

One of the important goals of the BCM project is to control the inherent fluctuations of PV technologies via the flexibility of BESS. Successful implementation of complex PV-battery control algorithms relies upon smart functionalities of inverters which, in turn, require that PV and BESS systems follow their setpoint command accurately. To this end, a variety of tests as part of the SAT are conducted by ComEd. This paper summarized the successful completion

of the P/Q priority test, the Volt/Var control test, and the power factor control test. Detailed analysis revealed that in these three tests, the BESS inverter successfully followed the given commands. Successful passing of SAT is a stepping stone to future work that will implement advanced algorithms via pertaining controllers in order to continuously maintain BCM operation in compliance with interconnection standards.

BIBLIOGRAPHY

- [1] A. Hirsch, Y. Parag and J. Guerrero, "Microgrids: A review of technologies, key drivers, and outstanding issues," *Renewable and Sustainable Energy Reviews*, vol. 90, pp. 402-411, July 2018.
- [2] S. Parhizi, H. Lotfi, A. Khodaei and S. Bahramirad, "State of the Art in Research on Microgrids: A Review,," *IEEE Access*, vol. 3, pp. 890-925, 2015.
- [3] A. Majzoobi, A. Khodaei, S. Bahramirad and M. Bollen, "Capturing the Variabilities of Distribution Network Net-Load via Available Flexibility of Microgrids," in *Grid of the Future Symposium (CIGRE)*, Philadelphia PA, 2016.
- [4] R. Sharma and S. Mishra, "Dynamic Power Management and Control of a PV PEM Fuel-Cell-Based Standalone ac/dc Microgrid Using Hybrid Energy Storage," *IEEE Transactions on Industry Applications*, vol. 54, no. 1, pp. 526-538, 2018.
- [5] H. Mahmood and J. Jiang, "Autonomous Coordination of Multiple PV/Battery Hybrid Units in Islanded Microgrids," *IEEE Transactions on Smart Grid*, vol. 9, no. 6, pp. 6359-6368, 2018.
- [6] Z. Yi, W. Dong and A. Etemadi, "A Unified Control and Power Management Scheme for PV-Battery-Based Hybrid Microgrids for Both Grid-Connected and Islanded Modes," *IEEE Transactions on Smart Grid*, vol. 9, no. 6, pp. 5975-5985, 2018.
- [7] ComEd, "Bronzeville Community of The Future," [Online]. Available: <https://bronzevillecommunityofthefuture.com/project-microgrid/>. [Accessed 13 July 2019].